Stem Cell Reports
Report
ISSCR
OPEN ACCESS

Programmatic introduction of parenchymal cell types into blood vessel organoids

Amir Dailamy,[1,5] Udit Parekh,[2,5] Dhruva Katrekar,[1] Aditya Kumar,[1] Daniella McDonald,[3] Ana Moreno,[1,4] Pegah Bagheri,[1] Tse Nga Ng,[2] and Prashant Mali[1,*]
[1]Department of Bioengineering, University of California San Diego, CA 92093, USA
[2]Department of Electrical and Computer Engineering, University of California San Diego, CA 92093, USA
[3]Biomedical Sciences Graduate Program, University of California San Diego, CA 92093, USA
[4]Present address: Navega Therapeutics, San Diego, CA 92121, USA
[5]These authors contributed equally
*Correspondence: pmali@ucsd.edu
https://doi.org/10.1016/j.stemcr.2021.08.014

SUMMARY

Pluripotent stem cell-derived organoids have transformed our ability to recreate complex three-dimensional models of human tissue. However, the directed differentiation methods used to create them do not afford the ability to introduce cross-germ-layer cell types. Here, we present a bottom-up engineering approach to building vascularized human tissue by combining genetic reprogramming with chemically directed organoid differentiation. As a proof of concept, we created neuro-vascular and myo-vascular organoids via transcription factor overexpression in vascular organoids. We comprehensively characterized neuro-vascular organoids in terms of marker gene expression and composition, and demonstrated that the organoids maintain neural and vascular function for at least 45 days in culture. Finally, we demonstrated chronic electrical stimulation of myo-vascular organoid aggregates as a potential path toward engineering mature and large-scale vascularized skeletal muscle tissue from organoids. Our approach offers a roadmap to build diverse vascularized tissues of any type derived entirely from pluripotent stem cells.

INTRODUCTION

The ability to recapitulate organogenesis and create complex human tissue *in vitro* has been a long-standing goal for the stem cell and tissue engineering field. The advent of organoid technology has recently made it possible to create three-dimensional (3D), self-organized, pluripotent stem cell (PSC)-derived tissues for *in vitro* developmental and disease modeling that closely mimic the cellular, spatial, and molecular architecture of endogenous human tissue (Clevers, 2016; Lancaster and Knoblich, 2014). These advances have enabled substantial progress in building fully PSC-derived, functional human organs *in vitro* (Takebe and Wells, 2019). However, the absence of vasculature in most organoid techniques limits their utility, principally in two ways. Firstly, it is widely accepted that vasculature plays a crucial role in development and disease (Daniel and Cleaver, 2019; Petrova and Koh, 2018). Secondly, vasculature is necessary to prevent necrosis in tissues that grow beyond 1 mm in size (Grebenyuk and Ranga, 2019; Lancaster, 2018), which deems vasculature critical for building large-scale tissue models.

To address this, several groups have demonstrated progress on developing methods for vascularizing organoids (Cakir et al., 2019; Garreta et al., 2019; Guye et al., 2016; Homan et al., 2019; Low et al., 2019; Mansour et al., 2018; Pham et al., 2018). Some groups have succeeded in vascularizing organoids after transplanting them *in vivo* (Mansour et al., 2018; Pham et al., 2018), but requiring an *in vivo* host limits experimental control, increases cost, and diminishes its potential for clinical applications. Others transiently overexpressed *GATA6* to introduce a nascent vascular network in liver-bud organoids (Guye et al., 2016); however, there is no current evidence this system can be translated to other organoids.

Organoid platforms leverage knowledge of development to provide temporally appropriate chemical cues to self-assembled PSC-derived embryoid bodies, modulating key organogenesis-specific signaling pathways to drive the directed differentiation of organ-specific cells in physiologically faithful architectures. Thus, cells that do not belong to those specific organ compartments or arise from different germ layers are absent from the final organoid. To introduce cell types outside of those available from directed differentiation, a promising strategy is to combine genetic overexpression with directed differentiation. Recently, vascularization of cerebral organoids has been reported, in which PSCs were engineered to ectopically express human ETS variant 2 (*ETV2*) (Cakir et al., 2019), a known driver of differentiation to endothelial cells from PSCs (Lindgren et al., 2015; Parekh et al., 2018). Although this method has exciting potential, it suffers from two limitations: one, it induces only a low degree of vascularization, and, two, it does not induce the full panoply of vascular lineages, such as smooth muscle cells (SMCs) and mesenchymal stem cells (MSCs), which are critical for blood vessel development and function (Ferland-McCollough et al., 2017). Thus, there is a need to explore alternative methods.

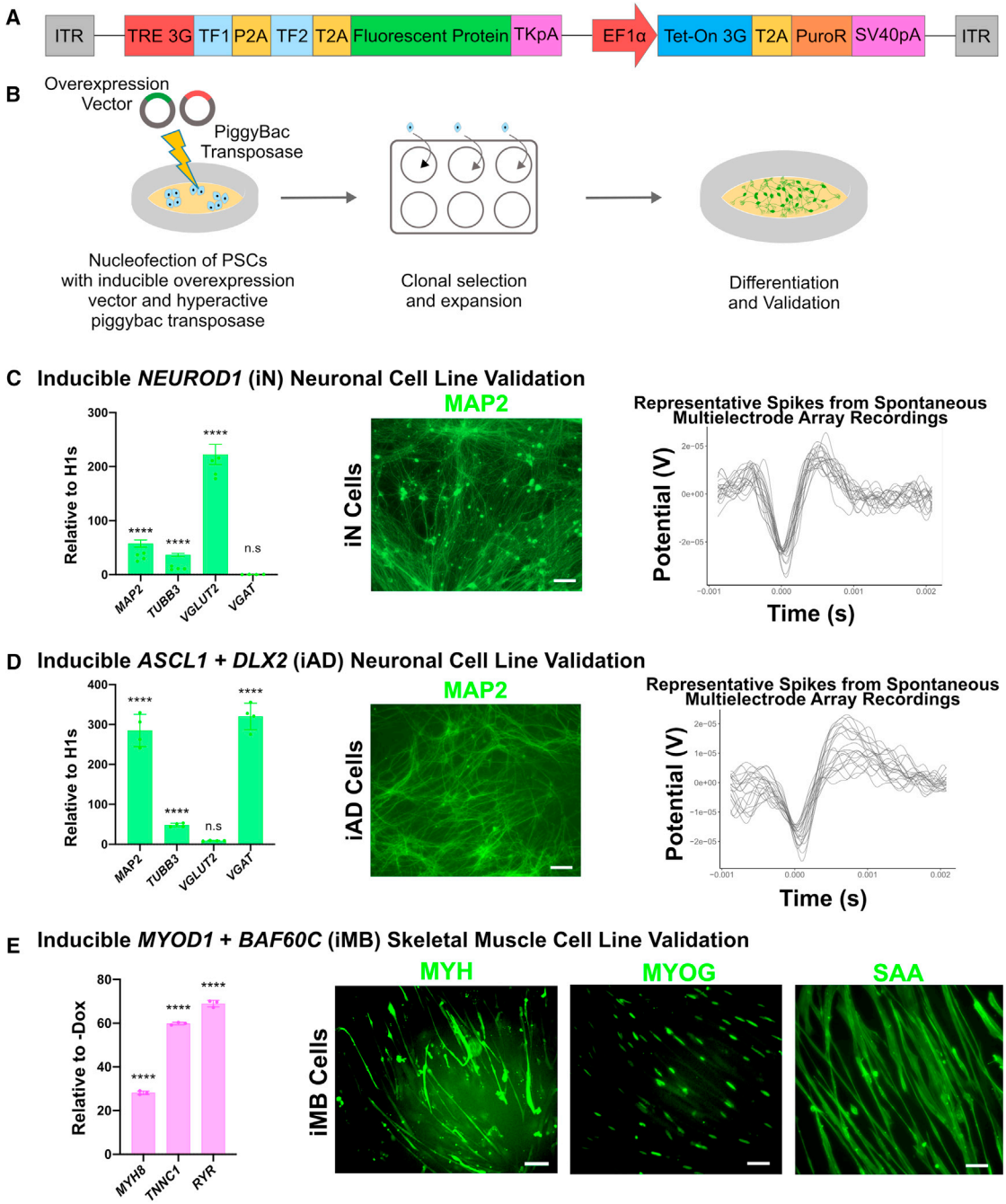

Figure 1. Construction and characterization of inducible cell lines

(A) Schematic of PiggyBac transposon-based inducible overexpression vector.

(B) Schematic of cell line generation and validation process.

(C) Inducible *NEUROD1* (iN) cell line validation at 3 weeks post induction via (1) qRT-PCR analysis of signature neuronal markers *MAP2*, *TUBB3*, *VGLUT2*, and *VGAT*; data represent the mean ± SD (n = 4 independent experiments); (2) immunofluorescence micrograph of *MAP2*+ cells (scale bars, 50 μm); and (3) representative spike plots from MEA measurements of spontaneously firing iN cells.

(D) Inducible *ASCL1+DLX2* (iAD) cell line validation at 3 weeks post induction via (1) qRT-PCR analysis of signature neuronal markers *MAP2*, *TUBB3*, *VGLUT2*, and *VGAT*; data represent the mean ± SD (n = 4 independent experiments); (2) immunofluorescence micrograph of *MAP2*+ cells (scale bars, 50 μm); and (3) representative spike plots from MEA measurements of spontaneously firing iAD cells.

(legend continued on next page)

A recently described vascular organoid (VO) differentiation approach (Wimmer et al., 2019) yields complete blood vessel networks, including SMCs, MSCs, and endothelial cells, but these organoids lack organ-specific parenchymal cells, limiting their utility for broader disease modeling and regenerative medicine. Here, we overlay reprogramming with the directed differentiation of VOs to derive cross-germ-layer and cross-lineage organoids with complete vascular networks. We introduce a parenchymal cell component into VOs via transcription factor (TF) overexpression and demonstrate this approach by building neuro-vascular and myo-vascular organoids. This is done by the induced overexpression, in developing vascular organoids, of *NEUROD1* (iN) to form neuro-vascular organoids (iN-VOs), and the induced overexpression of *MYOD1* plus *BAF60C* (iMB) to form myo-vascular organoids (iMB-VOs).

This yields a facile method for co-differentiation of tissue-specific parenchymal cells and the entire blood vessel lineage from a single PSC line. We present this approach as a proof of concept for the introduction of other parenchymal cell types, via the overexpression of lineage-specifying TFs, in the context of a VO scaffold.

RESULTS

Inducible cell line construction and validation

For the inducible expression of TFs, we designed a PiggyBac transposon-based overexpression vector that allowed a single vector to package the complete Tet-On system for doxycycline inducible expression, along with one or more TFs to be overexpressed in conjunction with a reporter fluorescent protein (Figure 1A). To establish the utility of our PiggyBac overexpression platform, we constructed an array of cell lines and validated their ability to differentiate into functional tissue upon adding doxycycline. For neural differentiation, we chose to overexpress *NEUROD1* to generate glutamatergic excitatory neurons (Parekh et al., 2018; Zhang et al., 2013), and *ASCL1+DLX2* for GABAergic inhibitory neuron differentiation (Yang et al., 2017). For mesodermal tissue differentiation, we chose to overexpress *MYOD1+BAF60C* (Albini et al., 2013) for skeletal muscle differentiation. Stable, dox-inducible *NEUROD1* (iN), *ASCL1+DLX2* (iAD), and *MYOD1+BAF60C* (iMB) human embryonic stem cell (hESC) lines were generated by nucleofecting hESCs with the respective overexpression vector, along with a hyperactive PiggyBac transposase (Yusa et al., 2011).

For validation of neural differentiation of iN and iAD lines, qRT-PCR analysis demonstrated upregulation of neuronal markers *MAP2* and *TUBB3* for both iN and iAD cells (Figures 1C and 1D) compared with undifferentiated hESCs. iN neurons were confirmed to be glutamatergic via upregulation of excitatory marker *VGLUT2* with no detectable expression of the inhibitory marker *VGAT* (Figure 1C), while iAD neurons were confirmed to be GABAergic, via upregulation of *VGAT* with minimal expression of *VGLUT2* (Figure 1D). *MAP2*+ cells with classic neuronal morphology were confirmed by immunofluorescence for both iN and iAD cells (Figures 1C and 1D). Finally, iN and iAD neurons were confirmed to be functional by detection of spontaneous firing when co-cultured with glia and measured on a microelectrode array (MEA) at 3–5 weeks post induction (Figures 1C and 1D).

Skeletal muscle differentiation of iMB cells was validated by gene expression and immunofluorescence assays (Figure 1E). qRT-PCR analysis confirmed upregulation of skeletal muscle markers *MYH8*, *TNNC1*, and *RYR*. Immunofluorescence confirmed the presence of characteristic spindle-shaped *MYH*+ and *SAA*+ skeletal muscle morphology, along with *MYOG*+ nuclei.

Constructing neuro-vascular and myo-vascular organoids

After clonal hESC lines were established, we developed a modular, generalizable, TF overexpression-based strategy to differentiate parenchymal cell types in VOs (Figure 2A). We conducted an optimization experiment (Note S1) to determine if wild-type ESCs are required for maintaining the vascular compartment in our organoids (Figure S1A). Given the higher expression of *MAP2* and comparable expression of *CDH5*, subsequent experiments were conducted with iN-VOs formed from 100% iN cells (Figure S1B). Immunostaining was performed on both induced (+dox, iN-VOs) and uninduced (−dox, iN-VOs) organoids, confirming *MAP2*+ cells forming into bundle-like structures of neurons only in induced organoids, along with dense, interpenetrating *CDH5*+ vascular networks in both conditions (Figure 2C). Furthermore, pan-organoid confocal images show that endothelial networks span all layers of the organoid, as do neurons, although they are not uniformly distributed and form clusters and bundles of cells (Figures 2G and S1C; Videos S1 and S3). Further analysis via qRT-PCR showed an upregulation of the excitatory marker *VGLUT2*, along with cortical neuron markers *BRN2* and *FOXG1* (Zhang et al., 2013) in day 15 iN-VOs (Figure 2D). Moreover, we observed expression levels comparable with uninduced organoids of the endothelial

(E) Inducible *MYOD1+BAF60C* (iMB) cell line validation at 2 weeks post induction via (1) qRT-PCR analysis of signature skeletal muscle markers *MYH8*, *TNNC1*, and *RYR*; data represent the mean ± SD (n = 3 independent experiments); and (2) immunofluorescence micrograph of *MYH*+-, *MYOG*+-, and *SAA*+-labeled cells (scale bars, 50 μm). (C–E) **p ≤ 0.01, ***p ≤ 0.001, and ****p ≤ 0.0001; ns, not significant.

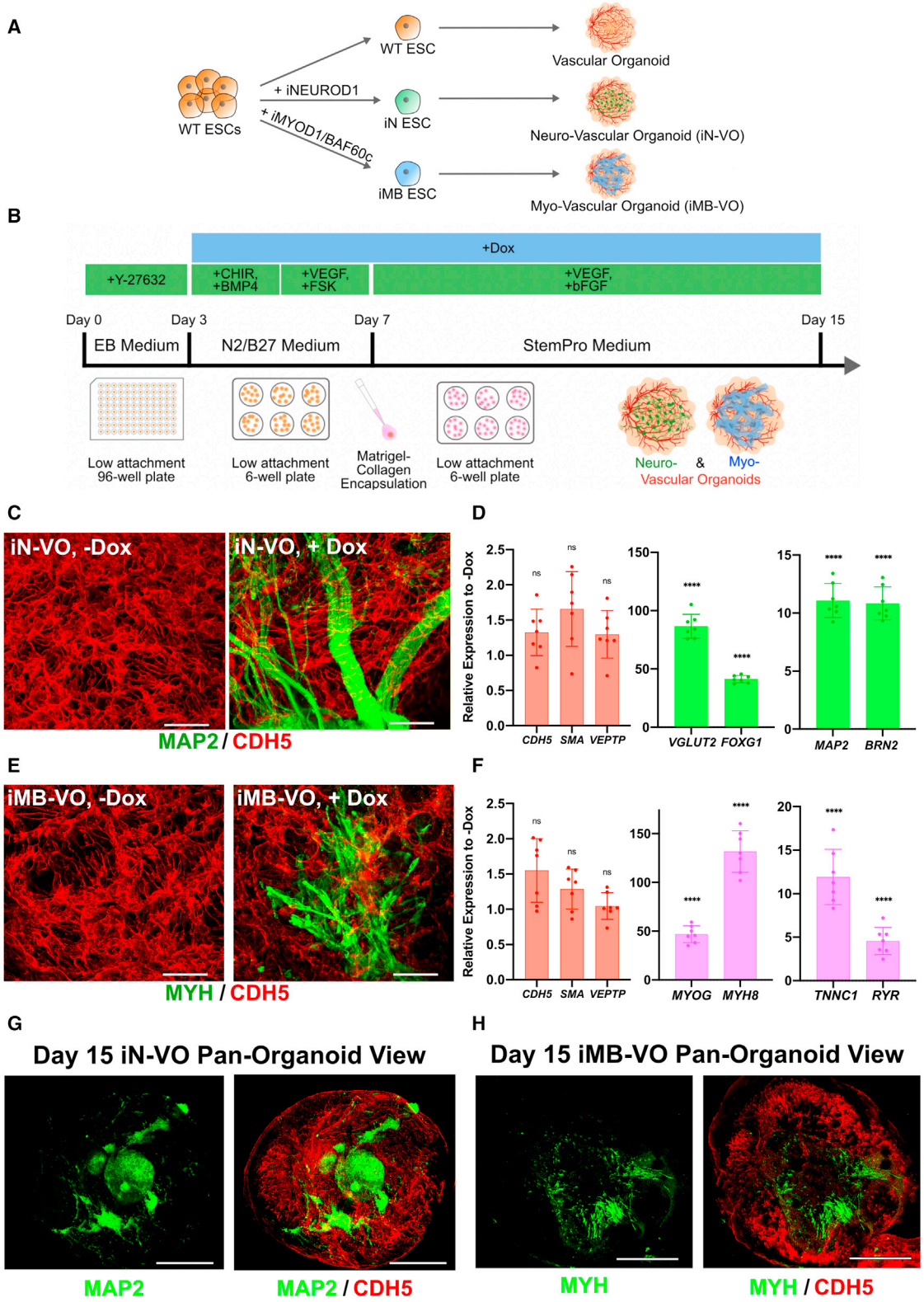

(legend on next page)

markers *CDH5* and *VEPTP*, along with the smooth muscle marker *SMA* (Figure 2D).

Once the formation of neuro-vascular organoids was established, we then sought to demonstrate if our system was compatible with other germ-layer or cross-lineage cell types. Using 100% iMB cells and the same protocol used to generate neuro-vascular organoids, we grew iMB-VOs (Figure 2B). iMB-VOs had *MYH*+ spindle-shaped cells (Figure 2E), along with expression of skeletal muscle marker genes *MYOG*, *MYH8*, *TNNC1*, and *RYR* (Figure 2F), confirming that our platform could also be used to grow vascularized tissue of mesodermal origin, specifically skeletal muscle. Pan-organoid tile-scan confocal images demonstrated *MYH*+ skeletal muscle cells present in many layers of the myo-vascular organoid, albeit not uniformly distributed throughout the organoid (Figures 2H and S1D; Videos S2 and S4).

Comprehensive characterization of neuro-vascular organoids

We then sought to enable further long-term culture of the neuro-vascular organoids beyond the initial 15 days (Figure S1E). Media optimization experiments (Note S2) revealed that brain-derived neurotrophic factor (BDNF) and neurotrophin-3 (NT-3) supplementation from day 15 ensured long-term survival of neurons with reliable maintenance of vascular lineages (Figure S1F).

Upon determining an optimized protocol for long-term growth of iN-VOs, we comprehensively characterized these long-term cultured neuro-vascular organoids (Figure 3A). qRT-PCR analysis showed an upregulation of the neuronal markers *MAP2*, *VGLUT2*, *BRN2*, and *FOXG1* in day 30 iN-VOs (Figure 3B), while maintaining the expression level of endothelial markers *CDH5* and *VEPTP*, and smooth muscle marker *SMA* (Figure 3B). Immunofluorescence imaging confirmed the presence of *MAP2*+ neurons displaying robust neurite growth, along with interpenetrating *CDH5*+ vascular networks through 30 days in culture (Figure 3C). These organoids formed capillary networks that consisted of lumen-forming endothelial cells (Figure S3A) that were tightly associated with pericytes (Figure 3D).

To characterize the cell-type composition of iN-VOs cultured for up to 45 days, we assayed them using single-cell RNA-sequencing (scRNA-seq). We assayed 26,959 cells across day 45 organoids grown under three conditions: 15 days of *NEUROD1* overexpression (iN-VO, 15 days induction), 45 days of *NEUROD1* overexpression (iN-VO, 45 days induction), and without overexpression (iN-VO, no induction). Using the Seurat pipeline (Butler et al., 2018), we identified that *PRRX1*+ mesenchymal progenitors, *MEOX2*+ differentiating pericytes, and cycling cells were present in all three types of organoids and constituted a majority of each of the organoids (Figures 3E, 3F, S2A, and S2B). Importantly, functional vascular cell types *PDGFRβ*+ pericytes and *PECAM1*+ endothelial cells were present in all types of organoids and constituted 16%–22% and 2.5%–6% of cells respectively (Figures 3E, 3F, S2A, and S2B). Endothelial and neural cells mapped with high fidelity to the endothelium and neurons from the Mouse Cell Atlas, respectively (Figure S2C). To further validate their identity, neurons from the neuro-vascular organoids were mapped to *DCX*+ neuronal clusters from a reference dataset profiling two-dimensional (2D) differentiation of neurons from hPSCs by NGN2 overexpression (Schörnig et al., 2021) (Figures S2D and S2E). After molecular characteristics of the iN-VOs were assayed, we assessed the functionality of both neural and vascular cell types in the organoid. First we assessed endothelial function *in vitro* by confirming uptake of acetylated low-density lipoprotein by endothelial cells in the organoids (Figure S3B). Further, we assayed

Figure 2. Generation of iN-VOs and iMB-VOs

(A) General strategy for the generation of vascularized organ tissues via introduction of parenchymal cell types in VOs.

(B) Schematic of iN-VO and iMB-VO culture protocol.

(C) Immunofluorescence 100-μm z stack, maximum projection, confocal micrographs of *MAP2*- and *CDH5*-labeled uninduced (iN-VO, −Dox) and induced (iN-VO, +Dox) day 15 iN-VO organoids (scale bars, 50 μm).

(D) qRT-PCR analysis of signature endothelial genes *CDH5* and *VEPTP*; signature smooth muscle gene *SMA*; and signature neuronal genes *MAP2*, *VGLUT2*, *BRN2*, and *FOXG1* at day 15 of culture for iN-VO organoids. Data represent the mean ± SD (n = 7 organoids, from three independent experiments).

(E) Immunofluorescence 100-μm z stack, maximum projection, confocal micrographs of *MYH*- and *CDH5*-labeled uninduced (iMB-VO, −Dox) and induced (iMB-VO, +Dox) day 15 iMB-VO organoids (scale bars, 50 μm).

(F) qRT-PCR analysis of signature endothelial genes *CDH5* and *VEPTP*; signature smooth muscle gene *SMA*; and signature skeletal muscle genes *MYOG*, *MYH8*, *TNNC1*, and *RYR* at day 15 of culture for iMB-VO organoids. Data represent the mean ± SD (n = 7 organoids, from three independent experiments).

(G) Pan-organoid tile-scan immunofluorescence confocal micrograph of a *CDH5*- and *MAP2*-labeled day 15 neuro-vascular organoid (scale bars, 500 μm). Image is a 200-μm z stack maximum intensity projection.

(H) Pan-organoid tile-scan immunofluorescence confocal micrograph of *CDH5*- and *MYH*-labeled day 15 myo-vascular organoid (scale bars, 500 μm). Image is a 200-μm z stack maximum intensity projection. (D and F) $^{**}p \leq 0.01$, $^{***}p \leq 0.001$, and $^{****}p \leq 0.0001$; ns, not significant.

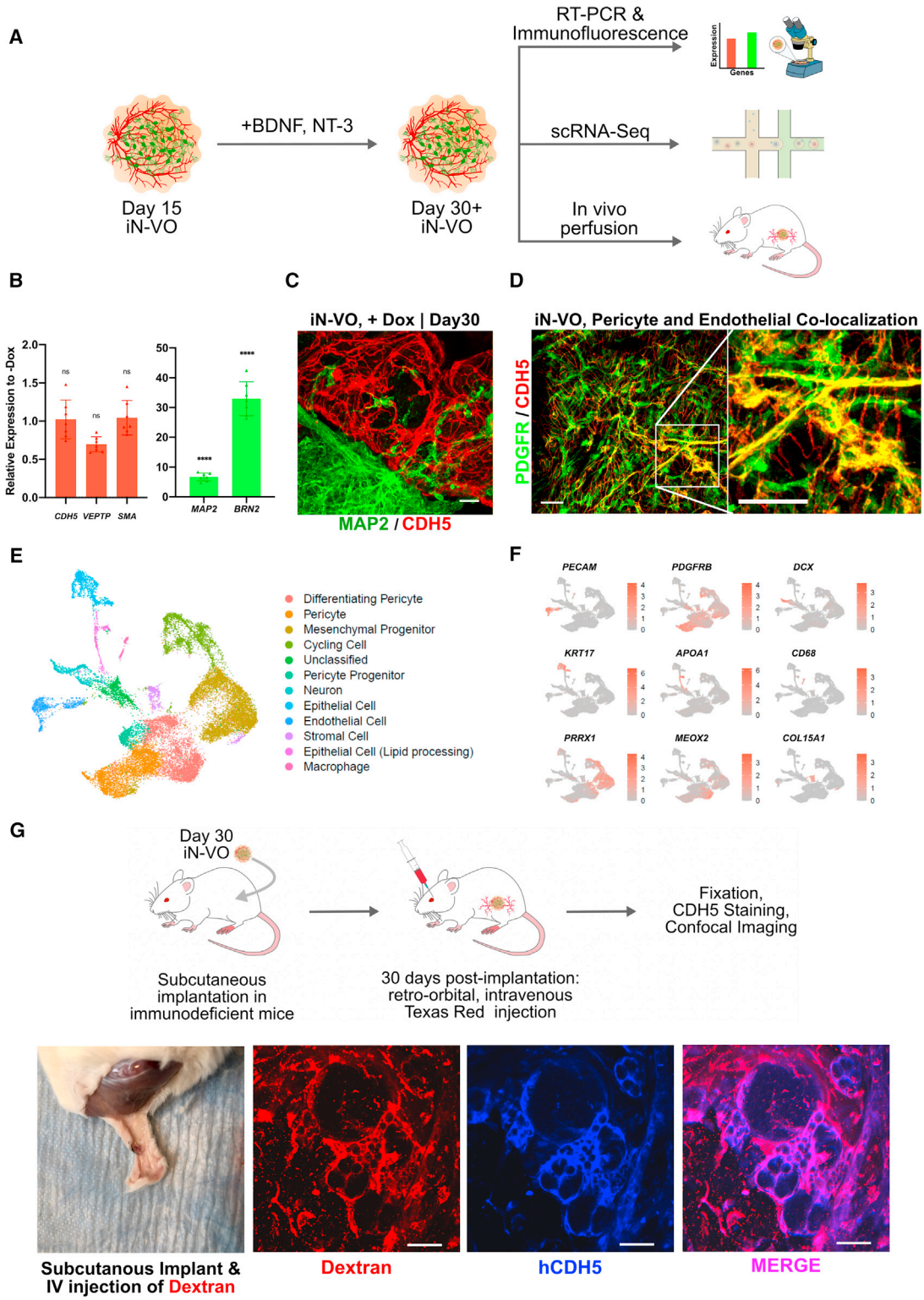

Figure 3. Molecular and functional characterization of iN-VOs

(A) Outline of long-term cultured iN-VO characterization.

(B) qRT-PCR analysis of signature endothelial genes *CDH5* and *VEPTP*, signature smooth muscle gene *SMA*, and signature neuronal genes *MAP2* and *BRN2* at day 30 of iN-VO culture. Data represent the mean ± SD (n = 7 organoids, from three independent experiments).

(legend continued on next page)

the ability of the vascular networks to form perfusable blood vessels when implanted into mice. Specifically, iN-VOs were grown till day 30 *in vitro*, and then subcutaneously implanted in Rag2$^{-/-}$;γc$^{-/-}$ immunodeficient mice. Thirty and 90 days post implantation, intravenous (IV) injection of a Texas red dye followed by organoid extraction, fixation, and immunofluorescence staining showed co-localization of the dye with human *CDH5*+ vascular cells and *PDGFR*+ pericytes in the iN-VO (Figures 3G and S3C). Endothelium function *in vivo* was sustained for at least 90 days post implantation, as demonstrated by confocal imaging of lumenized and perfused *CDH5*+ vessels (Figure S3Cii,iii). The absence of *CDH5* signal in wild-type mouse kidneys stained with human-specific anti-*CDH5* demonstrates the human specificity of the antibody (Figure S3D), confirming that the perfused *CDH5*+ vessels in the organoids are of human origin.

To assess functionality of neurons in the iN-VOs, we assayed the organoids for spontaneous electrical activity using MEAs (Figures 4A and 4B). Strikingly, while uninduced organoids displayed no spontaneous activity, spontaneous firing was repeatedly observed in iN-VOs (Figure 4C), confirming the presence of functional neurons. Taken together, we demonstrate the formation of functional neuro-vascular tissue with long-term culture capability.

In vitro maturation of myo-vascular organoids

Finally, while our iMB-VO platform was able to differentiate vascularized skeletal muscle, maturation of this lineage *in vitro* is a long-standing challenge. To further mature the differentiated skeletal muscle, we applied chronic electrical stimulation (Khodabukus et al., 2019; Rao et al., 2018).

To subject organoids to stimulation, we encapsulated them in a fibrin and Matrigel blend, and placed them in a custom chip between two graphite rods. A pulsed constant-voltage stimulation was then applied for a week after encapsulation to drive maturation (Figure 4D). Organoids were then assayed for gene expression of muscle and calcium-handling genes (Figure 4E). In stimulated organoids, embryonic skeletal muscle myosin (*MYH3*) was upregulated, along with a small increase in expression of adult fast skeletal muscle myosin (*MYH2*). Additionally, the calcium-handling genes *CASQ2* and *SERCA2* were also highly upregulated. In summary, our iMB-VO approach is a promising method to generate mature, vascularized skeletal muscle tissue *in vitro*.

DISCUSSION

In this work, we have demonstrated that a combination of directed differentiation and the overexpression of a lineage-specific reprogramming factor can build cross-lineage and cross-germ-layer organoid systems. We used this approach to introduce neurons and skeletal muscle into VOs, as a proof of principle of such an approach. We then assayed these mixed-lineage organoids to demonstrate that this combined approach yielded neurons only upon induction of *NEUROD1* overexpression, and skeletal muscle only upon induction of *MYOD1+BAF60C* overexpression, while retaining the architecture of the VO. The neuro-vascular organoids thus generated were further optimized for long-term culture, and comprehensively characterized for composition and to confirm function of both lineage branches. Finally, for the myo-vascular organoids, we demonstrated the maturation of these organoids via chronic electrical stimulation, which enhanced the expression of skeletal muscle myosins and calcium-handling genes.

While providing a modular and powerful approach to engineer vascularized multi-lineage organoids, several challenges still remain to be solved. While we have taken advantage of known reprogramming factors to differentiate neurons and skeletal muscle, such recipes are not known for all cell types and will have to be discovered. Known overexpression recipes may also need to be modified for organoid culture conditions, since recipes are typically optimized and validated only for specific 2D culture and media conditions. While we have restricted the current study to overexpression, knockdown approaches (Qian et al., 2020) may also be important tools in these engineering efforts. Additionally, improved control of this spatial organization will be critical for accurate tissue engineering, especially as reprogrammed cells transition directly from initial to final lineage states, and one may need to incorporate novel strategies like optogenetic control of gene expression (Nihongaki et al, 2015, 2017; Polstein and Gersbach, 2015) or synthetic biology approaches (Toda et al., 2018).

(C) Immunofluorescence 100-μm z stack, maximum projection, confocal micrographs of *MAP2*+- and *CDH5*+-induced day 30 iN-VOs (scale bars, 100 μm).

(D) Immunofluorescence100-μm z stack, maximum projection, confocal micrographs of *PDGFR*+-and *CDH5*+-induced day 30 iN-VOs (scale bars, 50 μm).

(E) Uniform manifold approximation and projection (UMAP) visualization of cell types from day 45 iN-VOs. Two independent induction conditions, along with one non-induction condition.

(F) Cluster-specific expression of marker genes in day 45 iN-VOs.

(G) Experimental validation of iN-VO perfusibility *in vivo* by subcutaneous implantation of iN-VO, showing immunofluorescence micrographs of intravital Dextran, *CDH5*, and overlay (scale bar, 25 μm). Representative image from two independent experiments.

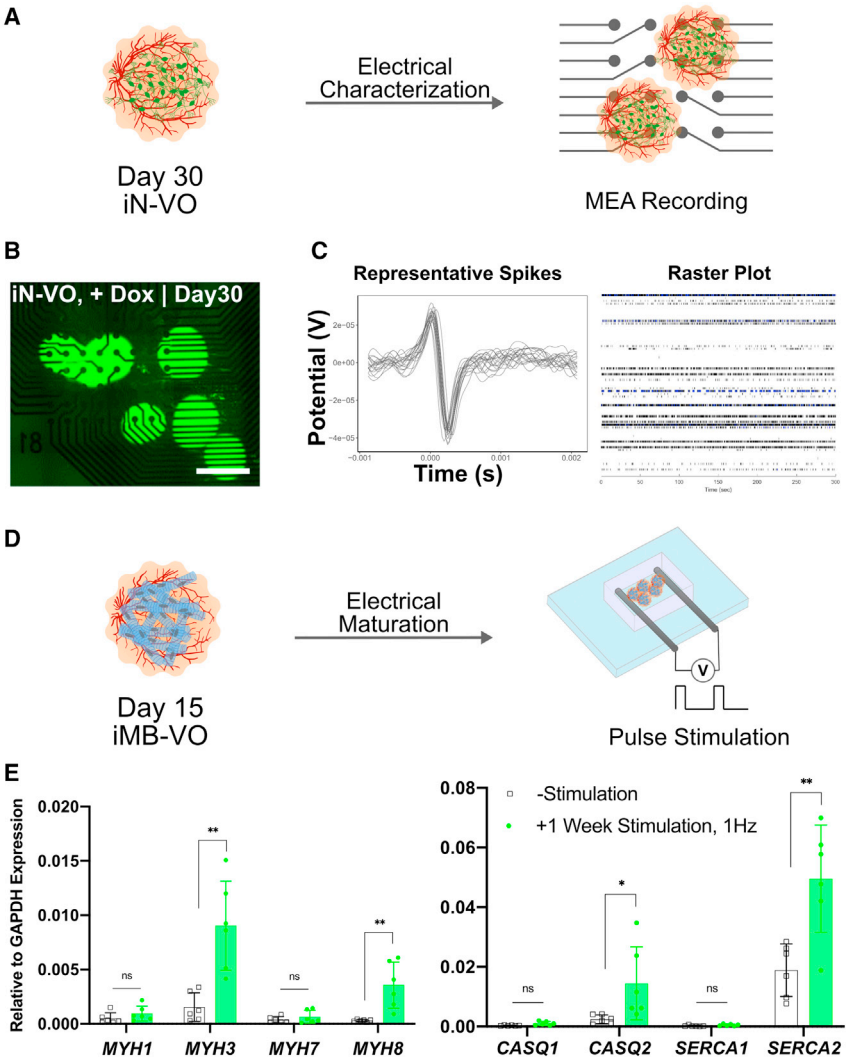

Figure 4. Electrical characterization and stimulation of organoids

(A) Schematic of iN-VO electrical characterization via MEA recordings.

(B) Image of day 30 iN-VOs plated on microelectrode array (scale bars, 500 μm).

(C) Representative spike plots from MEA measurements of spontaneously firing iN-VOs and corresponding raster plot. Representative image and plot from two independent experiments.

(D) Schematic of iMB-VO *in vitro* maturation by electrical stimulation.

(E) qRT-PCR analysis of skeletal muscle myosins: *MYH2*, *MYH3*, *MYH7*, and *MYH8*, and genes involved in calcium handling, *CASQ1*, *CASQ2*, *SERCA1*, *SERCA2*, and *RYR* for stimulated versus unstimulated iMB-VOs. Data represent the mean ± SD (n = 6 organoids, from two independent experiments). **p ≤ 0.01, ***p ≤ 0.001, and ****p ≤ 0.0001; ns, not significant.

In summary, our demonstrated approach provides a blueprint for complete bottom-up engineering of vascularized organoids, where genetic perturbation methods for cell reprogramming can be overlaid onto our core protocol to introduce additional cell types. This framework could be a powerful platform to generate diverse vascularized organoids, thus laying the foundation for completely *in vitro*-derived, large-scale tissue systems for regenerative medicine purposes.

EXPERIMENTAL PROCEDURES

Detailed methods are provided in the supplemental experimental procedures.

iMB-VO and iN-VO generation

To generate iMB-VOs or iN-VOs, 9,000 iMB or iN cells, respectively, were seeded in ULA 96 well plates for embryoid body (EB) formation. EBs were grown in EB media (DMEM/F12 + 20% KOSR + 50 μM Y-27632) for 2 days and then transferred into an ULA 6-well plate, with about 8–12 EBs/well. This media was then replaced with 2 mL of Mesoderm Induction Media (N2/B27 + BMP4 + CHIR), with the addition of doxycycline to introduce either the muscle or neural compartment for iMB-VOs or iN-VOs, respectively. Doxycycline was spiked into the media for every media change onwards. Organoids were then cultured at 37°C, 5% CO_2 for 3 days. Three days later, the medium was replaced with 2 mL of Vascular Induction Media (N2/B27 + VEGF + FSK) per well and cultured at 37°C, 5% CO_2. This media was replaced 24 hours later and cultured at 37°C, 5% CO_2 for 24 h. On day 7 of organoid formation, organoids were encapsulated in a blend of matrigel and collagen and then cultured in Vascular Maturation Media (StemPro + 15% FBS + VEGF + bFGF). Organoids were cultured at 37°C, 5% CO_2 and Vascular Maturation Media was replaced every 3 days. For long-term growth of iN-VOs, Vascular Maturation Media was supplemented with BDNF and NT-3 from day 15 and onwards.

Data and code availability

All scRNA-seq data can be accessed via GEO (GEO: GSE164268).

SUPPLEMENTAL INFORMATION

Supplemental information can be found online at https://doi.org/10.1016/j.stemcr.2021.08.014.

AUTHOR CONTRIBUTIONS

Conceptualization and design, A.D., U.P., T.N.N., and P.M.; experiments, A.D., U.P., D.K., A.K., D.M., A.M., and P.B.; computational analyses, U.P.; writing, A.D., U.P., and P.M., with input from all authors.

CONFLICT OF INTERESTS

A.D., U.P., and P.M. have filed patents based on this work. P.M. is a scientific co-founder of Shape Therapeutics, Boundless Biosciences, Navega Therapeutics, and Engine Biosciences, which have no commercial interests related to this study. The terms of these arrangements have been reviewed and approved by the University of California, San Diego, in accordance with its conflict of interest policies.

ACKNOWLEDGMENTS

The authors would like to thank James Yen, Yan Wu, Kian Kalhor, Reinner Wimmer, Cleber Trujillo, Hammza Khaliq, and Ramin Dailamy for useful discussions and support throughout all stages of the study; and Jennifer Santini from UCSD School of Medicine Microscopy Core (grant P30 NS047101). This work was generously supported by UCSD Institutional Funds and NIH grants (R01HG 009285, RO1CA222826, RO1GM123313). This publication includes data generated at the UCSD IGM Genomics Center utilizing an Illumina NovaSeq 6000 that was purchased with funding from an NIH SIG grant (S10 OD026929).

Received: January 5, 2021
Revised: August 22, 2021
Accepted: August 23, 2021
Published: September 23, 2021

REFERENCES

Albini, S., Coutinho, P., Malecova, B., Giordani, L., Savchenko, A., Forcales, S.V., and Puri, P.L. (2013). Epigenetic reprogramming of human embryonic stem cells into skeletal muscle cells and generation of contractile myospheres. Cell Rep. *3*, 661–670.

Butler, A., Hoffman, P., Smibert, P., Papalexi, E., and Satija, R. (2018). Integrating single-cell transcriptomic data across different conditions, technologies, and species. Nat. Biotechnol. *36*, 411–420.

Cakir, B., Xiang, Y., Tanaka, Y., Kural, M.H., Parent, M., Kang, Y.-J., Chapeton, K., Patterson, B., Yuan, Y., He, C.-S., et al. (2019). Engineering of human brain organoids with a functional vascular-like system. Nat. Methods *16*, 1169–1175.

Clevers, H. (2016). Modeling development and disease with organoids. Cell *165*, 1586–1597.

Daniel, E., and Cleaver, O. (2019). Vascularizing organogenesis: lessons from developmental biology and implications for regenerative medicine. Curr. Top. Dev. Biol. *132*, 177–220.

Ferland-McCollough, D., Slater, S., Richard, J., Reni, C., and Mangialardi, G. (2017). Pericytes, an overlooked player in vascular pathobiology. Pharmacol. Ther. *171*, 30–42.

Garreta, E., Prado, P., Tarantino, C., Oria, R., Fanlo, L., Martí, E., Zalvidea, D., Trepat, X., Roca-Cusachs, P., Gavaldà-Navarro, A., et al. (2019). Fine tuning the extracellular environment accelerates the derivation of kidney organoids from human pluripotent stem cells. Nat. Mater. *18*, 397–405.

Grebenyuk, S., and Ranga, A. (2019). Engineering organoid vascularization. Front. Bioeng. Biotechnol. *7*, 39.

Guye, P., Ebrahimkhani, M.R., Kipniss, N., Velazquez, J.J., Schoenfeld, E., Kiani, S., Griffith, L.G., and Weiss, R. (2016). Genetically engineering self-organization of human pluripotent stem cells into a liver bud-like tissue using Gata6. Nat. Commun. *7*, 10243.

Homan, K.A., Gupta, N., Kroll, K.T., Kolesky, D.B., Skylar-Scott, M., Miyoshi, T., Mau, D., Valerius, M.T., Ferrante, T., Bonventre, J.V., et al. (2019). Flow-enhanced vascularization and maturation of kidney organoids in vitro. Nat. Methods *16*, 255–262.

Khodabukus, A., Madden, L., Prabhu, N.K., Koves, T.R., Jackman, C.P., Muoio, D.M., and Bursac, N. (2019). Electrical stimulation increases hypertrophy and metabolic flux in tissue-engineered human skeletal muscle. Biomaterials *198*, 259–269.

Lancaster, M.A. (2018). Brain organoids get vascularized. Nat. Biotechnol. *36*, 407–408.

Lancaster, M.A., and Knoblich, J.A. (2014). Organogenesis in a dish: modeling development and disease using organoid technologies. Science *345*, 1247125.

Lindgren, A.G., Veldman, M.B., and Lin, S. (2015). ETV2 expression increases the efficiency of primitive endothelial cell derivation from human embryonic stem cells. Cell Regen. *4*, 1.

Low, J.H., Li, P., Chew, E.G.Y., Zhou, B., Suzuki, K., Zhang, T., Lian, M.M., Liu, M., Aizawa, E., Rodriguez Esteban, C., et al. (2019). Generation of human PSC-derived kidney organoids with patterned nephron segments and a de novo vascular network. Cell Stem Cell *25*, 373–387.e9.

Mansour, A.A., Gonçalves, J.T., Bloyd, C.W., Li, H., Fernandes, S., Quang, D., Johnston, S., Parylak, S.L., Jin, X., and Gage, F.H. (2018). An in vivo model of functional and vascularized human brain organoids. Nat. Biotechnol. *36*, 432–441.

Nihongaki, Y., Yamamoto, S., Kawano, F., Suzuki, H., and Sato, M. (2015). CRISPR-Cas9-based photoactivatable transcription system. Chem. Biol. *22*, 169–174.

Nihongaki, Y., Furuhata, Y., Otabe, T., Hasegawa, S., Yoshimoto, K., and Sato, M. (2017). CRISPR-Cas9-based photoactivatable transcription systems to induce neuronal differentiation. Nat. Methods *14*, 963–966.

Parekh, U., Wu, Y., Zhao, D., Worlikar, A., Shah, N., Zhang, K., and Mali, P. (2018). Mapping cellular reprogramming via pooled overexpression screens with paired fitness and single-cell RNA-sequencing readout. Cell Syst. *7*, 548–555.e8.

Petrova, T.V., and Koh, G.Y. (2018). Organ-specific lymphatic vasculature: from development to pathophysiology. J. Exp. Med. *215*, 35–49.

Pham, M.T., Pollock, K.M., Rose, M.D., Cary, W.A., Stewart, H.R., Zhou, P., Nolta, J.A., and Waldau, B. (2018). Generation of human vascularized brain organoids. Neuroreport *29*, 588–593.

Polstein, L.R., and Gersbach, C.A. (2015). A light-inducible CRISPR-Cas9 system for control of endogenous gene activation. Nat. Chem. Biol. *11*, 198–200.

Qian, H., Kang, X., Hu, J., Zhang, D., Liang, Z., Meng, F., Zhang, X., Xue, Y., Maimon, R., Dowdy, S.F., et al. (2020). Reversing a model of Parkinson's disease with in situ converted nigral neurons. Nature *582*, 550–556.

Rao, L., Qian, Y., Khodabukus, A., Ribar, T., and Bursac, N. (2018). Engineering human pluripotent stem cells into a functional skeletal muscle tissue. Nat. Commun. *9*, 126.

Schörnig, M., Ju, X., Fast, L., Ebert, S., Weigert, A., Kanton, S., Schaffer, T., Nadif Kasri, N., Treutlein, B., Peter, B.M., et al. (2021). Comparison of induced neurons reveals slower structural and functional maturation in humans than in apes. eLife *10*, e59323.

Takebe, T., and Wells, J.M. (2019). Organoids by design. Science *364*, 956–959.

Toda, S., Blauch, L.R., Tang, S.K.Y., Morsut, L., and Lim, W.A. (2018). Programming self-organizing multicellular structures with synthetic cell-cell signaling. Science *361*, 156–162.

Wimmer, R.A., Leopoldi, A., Aichinger, M., Wick, N., Hantusch, B., Novatchkova, M., Taubenschmid, J., Hämmerle, M., Esk, C., Bagley, J.A., et al. (2019). Human blood vessel organoids as a model of diabetic vasculopathy. Nature *565*, 505–510.

Yang, N., Chanda, S., Marro, S., Ng, Y.-H., Janas, J.A., Haag, D., Ang, C.E., Tang, Y., Flores, Q., Mall, M., et al. (2017). Generation of pure GABAergic neurons by transcription factor programming. Nat. Methods *14*, 621–628.

Yusa, K., Zhou, L., Li, M.A., Bradley, A., and Craig, N.L. (2011). A hyperactive piggyBac transposase for mammalian applications. Proc. Natl. Acad. Sci. U S A *108*, 1531–1536.

Zhang, Y., Pak, C., Han, Y., Ahlenius, H., Zhang, Z., Chanda, S., Marro, S., Patzke, C., Acuna, C., Covy, J., et al. (2013). Rapid single-step induction of functional neurons from human pluripotent stem cells. Neuron *78*, 785–798.

Stem Cell Reports, Volume *16*

Supplemental Information

Programmatic introduction of parenchymal cell types into blood vessel organoids

Amir Dailamy, Udit Parekh, Dhruva Katrekar, Aditya Kumar, Daniella McDonald, Ana Moreno, Pegah Bagheri, Tse Nga Ng, and Prashant Mali

SUPPLEMENTARY INFORMATION

Programmatic Introduction of Parenchymal Cell Types into Blood Vessel Organoids

Amir Dailamy[*,a], Udit Parekh*[*,b], Dhruva Katrekar[a], Aditya Kumar[a], Daniella McDonald[c], Ana Moreno[a,d], Pegah Bagheri[a], Tse Nga Ng[b], Prashant Mali*[†,a]

[a]*Department of Bioengineering, University of California San Diego, CA 92093, USA.*

[b]*Department of Electrical and Computer Engineering, University of California San Diego, CA 92093, USA.*

[c]*Biomedical Sciences Graduate Program, University of California San Diego, CA 92093, USA.*

[d]*Present address: Navega Therapeutics, San Diego, CA 92121, USA.*

**These authors contributed equally.* [†]*Correspondence: pmali@ucsd.edu.*

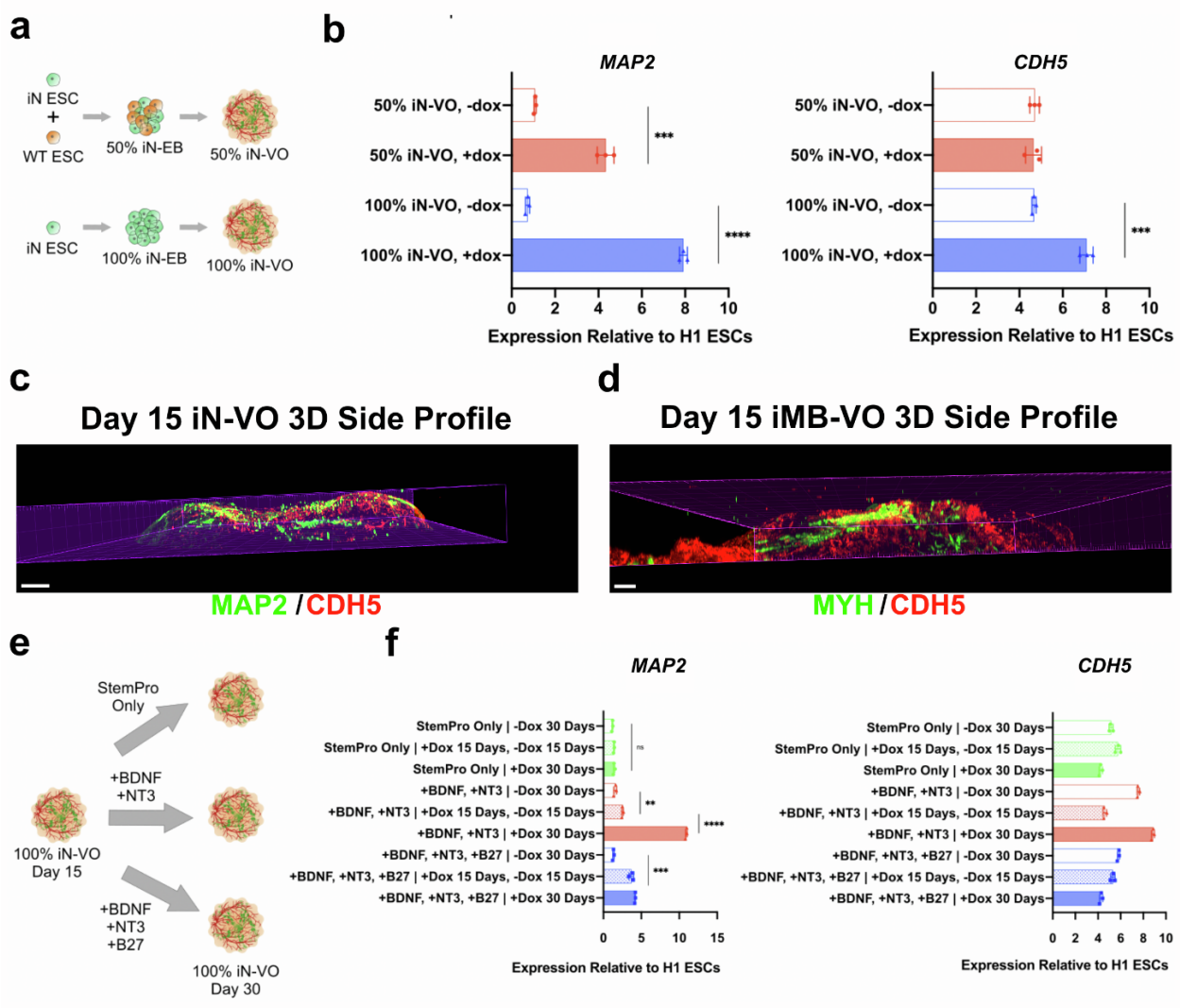

Figure S1: **Optimization of organoid culture conditions. (a)** Schematic for experiment to assess the optimal ratio of iN to WT cells for iN-VO formation. **(b)** qRT-PCR analysis of signature neuronal gene *MAP2*, and signature endothelial gene *CDH5*, at day 15 of culture for organoids grown from 50% and 100% iN cells. Data represent the mean ± s.d. (n = 3 organoids) and the unpaired two-tailed t-test was used for all comparisons. **(c)** Side profile 3D rendering of a pan-organoid tile-scan, z-stack immunofluorescence confocal micrograph of a *CDH5*- and *MAP2*-labelled day 15 neuro-vascular organoid (Scale bars = 150 µm). **(d)** Side profile 3D rendering of a pan-organoid tile-scan, z-stack immunofluorescence confocal micrograph of *CDH5*- and *MYH*-labelled day 15 myo-vascular organoid (Scale bars = 150 µm).**(e)** Schematic for experiment to

assess optimal media supplements for long term iN-VO culture. **(f)** qRT-PCR analysis of signature neuronal gene *MAP2*, and signature endothelial gene *CDH5*, at day 30 of culture to assess long term neuronal and endothelial survival. Data represent the mean ± s.d. (n = 3 organoids) and the unpaired two-tailed t-test was used for all comparisons. **(b,f)** Statistical significance was attributed to $P < 0.05$ as determined by unpaired two-tailed t-test comparisons. (**$P \leq 0.01$, ***$P \leq 0.001$, and ****$P \leq 0.0001$; ns = not significant).

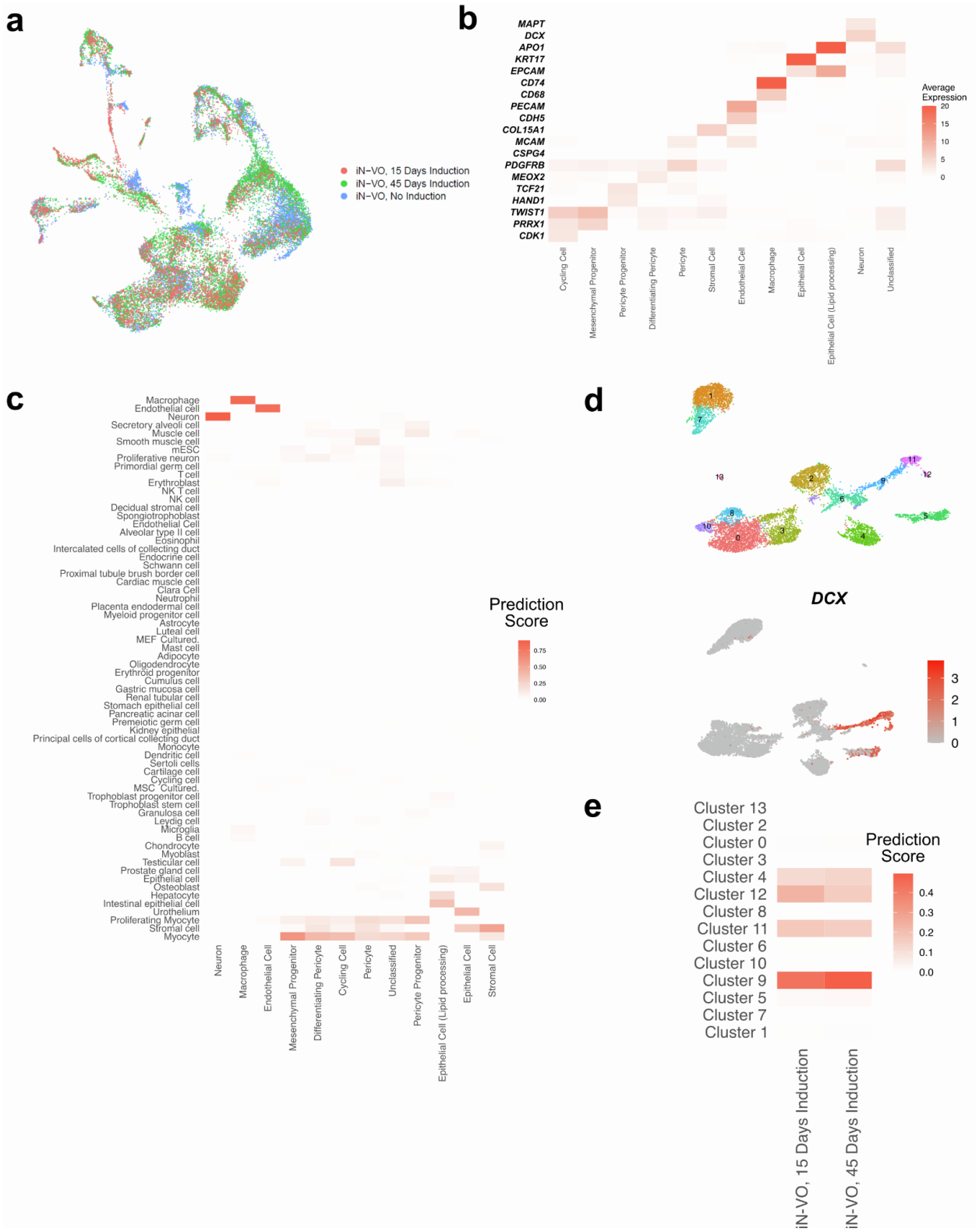

Figure S2: **scRNA-seq characterization of neurovascular organoids. (a)** UMAP visualization of iN-VO clusters annotated by sample type. Two independent induction conditions, along with

one non-induction condition. **(b)** Expression of marker genes for each classified cell type. **(c)** Mapping of neurovascular organoid cell types to cell types in the mouse cell atlas (Han et al. 2018). (**d**) UMAP visualization of clusters from a reference dataset of cells profiled during 2D differentiation of neurons from pluripotent stem cells by *NGN2* overexpression (Schörnig et al. 2021). Cells were profiled at day 14 and day 35 after induction. Neuronal clusters in the 2D differentiated neurons are highlighted below by overlaying *DCX* expression on the UMAP visualization. (**e**) Mapping of neurovascular organoid neurons to clusters in the 2D differentiated neurons.

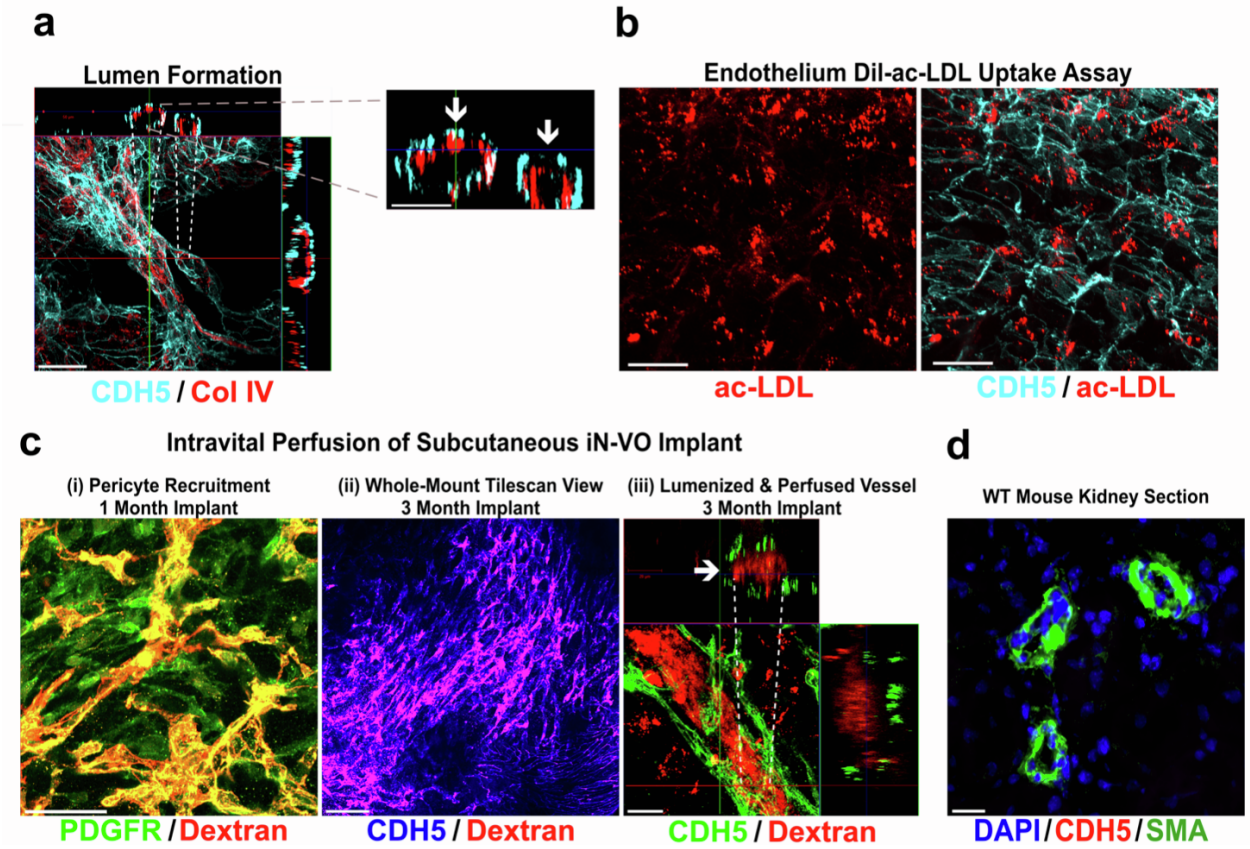

Figure S3: Extensive molecular and phenotypic characterization of long-term cultured iN-VOs. (a) The left image shows orthogonal sections of confocal stacks from neruo-vascular organoids stained for *CDH5* (red) and *Col IV* (Scale bars = 50 μm). The right image shows a zoomed in view of formed lumens, as indicated with arrowheads (Scale bars = 25 μm). **(b)** Immunofluorescence 100 μm z-stack, maximum projection, confocal micrographs of Day 30 neuro-vascular organoids labelled for *CDH5* post Dil-ac-LDL endothelial uptake assay (Scale bars = 50 μm). **(c)** Further characterization of endothelial functionality *in vivo* via intravital perfusion shows: (i) Experimental validation of pericyte recruitment of *in vivo* perfused neuro-vascular organoids, showing immunofluorescence micrograph of intravital Dextran and *PDGFRB* overlay (Scale bar = 50 μm); (ii) 100 μm z-stack projection that spans a 650 x 650 μm tilescan region of whole-mount neuro-vascular organoid implant showing intravital Dextran and *CDH5* overlay (Scale bar = 100 μm); and (iii) Orthogonal sections of confocal stacks from neuro-vascular organoids implants 90 days post-implantation, stained for *CDH5* (green) and showing dextran

perfused within the vessel. Lumens are indicated with arrowheads (Scale bars = 20 μm). **(d)** Wild-type mouse kidney stained for human-specific anti-*CDH5* and anti-*SMA* antibodies. Note the absence of the *CDH5* signal (Scale bar = 10 μm).

SUPPLEMENTAL MULTIMEDIA FILES

Supplemental Movie 1: 200 µm Z-stack playback of a day 15 neuro-vascular organoid confocal tile-scan micrograph. Organoid is stained for *CDH5* (red) and *MAP2* (green).

Supplemental Movie 2: 200 µm Z-stack playback of a day 15 myo-vascular organoid confocal tile-scan micrograph. Organoid is stained for *CDH5* (red) and *MYH* (green).

Supplemental Movie 3: 3D rendering of 200 µm Z-stack confocal tile-scan micrograph of a day 15 neuro-vascular organoid. Organoid is stained for *CDH5* (red) and *MAP2* (green). (Scale bar = 100 µm)

Supplemental Movie 4: 3D rendering of 200 µm Z-stack confocal tile-scan micrograph of a day 15 myo-vascular organoid. Organoid is stained for *CDH5* (red) and *MYH* (green). (Scale bar = 100 µm)

SUPPLEMENTAL EXPERIMENTAL PROCEDURES

Plasmid Construction

The piggyBac transposon plasmids for inducible overexpression of TFs were constructed using the backbone from 138-dCas9-Dnmt3a (Addgene Plasmid #84570) (Liu et al. 2016). The backbone plasmid was digested with NdeI and NsiI to remove the neomycin resistance cassette and was replaced with a puromycin resistance cassette using multi-element Gibson assembly. This puromycin resistant plasmid was then digested with NheI and AgeI to remove the dCas9-DNMT3A fusion sequence and replaced with the TF and fluorescent protein sequences separated by 2A peptide sequences using a multi-element Gibson assembly. TF and fluorescent protein sequences were amplified from plasmids: EF1a_NEUROD1_P2A_Hygro_Barcode (Addgene Plasmid #120466), EF1a_ASCL1_P2A_Hygro_Barcode (Addgene Plasmid #120427), phDLX2_N174 (Addgene Plasmid #60860) (Victor et al. 2014), EF1a_MYOD1_P2A_Hygro_Barcode (Addgene Plasmid #120464), pBS-hBAF60C (Addgene Plasmid #21036) (Wang et al. 1996), EF1a_mCherry_P2A_Hygro_Barcode (Addgene Plasmid #120426), and pEGIP (Addgene Plasmid #26777).

To construct a plasmid expressing the hyperactive piggyBac transposase (Yusa et al. 2011), the sequence for the enzyme was obtained as a synthesized double-stranded DNA fragment (Integrated DNA Technologies). This was cloned into an in-house plasmid using Gibson assembly, such that the expression of the transposase is driven by a CAG promoter.

The Gibson assembly reactions were set up as follows: 100 ng digested backbone, 3:10 molar ratio of insert, 2X Gibson assembly master mix (New England Biolabs), H_20 up to 20 µl. After incubation at 50 °C for 1 h, the product was transformed into One Shot Stbl3 chemically competent Escherichia coli (Invitrogen). A fraction (150 µL) of cultures was spread on carbenicillin (50 µg/ml) LB plates and incubated overnight at 37 ºC. Individual colonies were picked, introduced into 5 ml

of carbenicillin (50 µg/ml) LB medium and incubated overnight in a shaker at 37 ºC. The plasmid DNA was then extracted with a QIAprep Spin Miniprep Kit (Qiagen), and Sanger sequenced to verify correct assembly of the vector. Following verification of the vector, larger amounts of plasmid were obtained by seeding 150 µl of bacterial stock into 150 ml of LB medium containing carbenicillin (50 µg/ml) and incubating overnight in a shaker at 37 ºC for 16-18 h. The plasmid DNA was then extracted using a Plasmid Maxi Kit (Qiagen).

Cell Culture

H1 hESCs were maintained under feeder-free conditions in mTeSR1 medium (Stem Cell Technologies). Prior to passaging, tissue-culture plates were coated with growth factor-reduced Matrigel (Corning) diluted in DMEM/F-12 medium (Thermo Fisher Scientific) and incubated for 30 minutes at 37 ºC, 5% CO_2. Cells were dissociated and passaged using the dissociation reagent Versene (Thermo Fisher Scientific).

Generation of Clonal Inducible Overexpression Lines

hESC cells at 50-75% confluency from 3 wells of a 6-well plate were passaged using Versene. The cells were spun at 300 rcf for 5 minutes to obtain a cell pellet and this pellet was resuspended in a buffer containing 100 µl of P3 Nucleofector Solution (Lonza) and up to a maximum of 15 µl of a 1:1 mix of transposon vector plasmid to transposase plasmid by mass. This solution was loaded into a single Nucleovette (Lonza) and electroporated using the CB-150 pulse program on the 4D Nucleofector system (Lonza). After nucleofector run completion, 500 µl of pre-warmed mTeSR1 containing 10 µM Y27632 (Tocris Bioscience) was added to the Nucleovette and incubated at room temperature for 5 minutes. The cells were then removed from the Nucleovette using a Pasteur pipette and transferred dropwise into a 10 cm plate coated with growth-factor

reduced Matrigel as previously described and containing pre-warmed mTeSR1 with 10 μM Y27632.

Medium was then changed daily, and 48 hours after nucleofection cells were maintained under puromycin (Thermo Fisher Scientific) selection at 0.75 μg/ml. After approximately 7-10 days of culture post-nucleofection, colonies were large enough for clonal selection. To pick clonal lines, cells were treated with Versene for 3 minutes, Versene was aspirated and the plate was filled with DMEM/F-12 with 1% antibiotic-antimycotic (Thermo Fisher Scientific). Individual colonies were then carefully scraped under a microscope and transferred into individual wells of a 24-well plate coated with growth-factor reduced Matrigel and containing pre-warmed mTeSR1. These individually picked clones were expanded, aliquots were frozen in mFreSR (Stemcell Technologies) and validated by differentiation to relevant cell types. One validated clone from each line was chosen for further experiments. All clones were maintained in mTeSR1 under selection with puromycin at 0.75 μg/ml.

2D Differentiation of Inducible Overexpression hESC lines

Clonal lines overexpressing *NEUROD1* were differentiated following a previously described protocol (Zhang et al. 2013). Briefly, cells were passaged as single cells using Accutase (Innovative Cell Technologies) and plated in mTeSR1 at a density of 4-5x10^5 cells per well of a 6-well plate. The following day medium was changed to DMEM/F12 containing N2 supplement (Thermo Fisher Scientific), MEM non-essential amino acids (Thermo Fisher Scientific), 0.2 μg/ml mouse laminin (Invitrogen), 10 ng/ml BDNF (Peprotech), 10 ng/ml NT3 (Peprotech), 0.75 μg/ml puromycin and 1 μg/ml doxycycline (Sigma Aldrich) and cells were maintained in this medium for 2 days. On day 3 of differentiation cells were re-plated on Matrigel coated wells along with mouse glial cells in Neurobasal medium (Thermo Fisher Scientific) containing Glutamax (Thermo Fisher

Scientific), B27 supplement (Thermo Fisher Scientific), 10 ng/ml BDNF, 10 ng/ml NT3 and 1 µg/ml doxycycline. From day 5 onward, 2 µM Ara-c (Sigma Aldrich) was added to the medium to inhibit astrocyte proliferation. 50% of the medium was subsequently changed every 2-3 days. Cells were maintained in culture for up to 3 weeks. For functional characterization and electrical measurements, cells were plated on Matrigel coated 6-well multi-electrode arrays (Axion Biosystems) with mouse glial cells and maintained in culture for up to 3 weeks.

Clonal lines overexpressing *ASCL1* and *DLX2* were differentiated following a previously described protocol (Yang et al. 2017). Briefly, cells were passaged as single cells using Accutase (Innovative Cell Technologies) and plated in mTeSR1 at a density of 4-5x10^5 cells per well of a 6-well plate. The following day medium was changed to DMEM/F12 containing N2 supplement, MEM non-essential amino acids, 0.75 µg/ml puromycin and 1 µg/ml doxycycline and cells were maintained in this medium for 7-8 days, with the medium being changed every 2-3 days. 2 µM Ara-C was added to the medium on day 5 of differentiation. On day 7-8, the cells were passaged with Accutase and re-plated on Matrigel coated plates at a density of 4x10^5 cells per well of a 6-well plate in Neurobasal medium containing Glutamax, B27 supplement, 2 µM Ara-c and 1 µg/ml doxycycline. 50% of the medium was subsequently changed every 2-3 days. From day 15 onwards, medium was supplemented with 20 ng/ml BDNF and doxycycline was removed. For functional characterization and electrical measurements, cells were plated on Matrigel coated 6-well multi-electrode arrays (Axion Biosystems) with mouse glial cells and maintained in culture for up to 5 weeks.

Clonal lines overexpressing *MYOD* and *BAF60C* were differentiated to skeletal muscle following a process similar to a previously described protocol (Albini et al. 2013). Briefly, cells were passaged as single cells using Accutase and plated at a density of 4-5x10^5 cells per well of a 6-well plate. The following day, medium was changed to DMEM/F12 containing 15% fetal bovine serum (FBS, Thermo Fisher Scientific) and 1% anti-anti (Thermo Fisher Scientific). Medium was

exchanged every 2 days. On day 5 of differentiation, medium was changed to DMEM/F12 containing 2% horse serum (Hyclone) and 1% anti-anti. Differentiating cells were cultured for 3 weeks.

iMB-VO and iN-VO Generation

hESCs were grown in one well of a 6-well plate till they were 80% confluent. This was sufficient to seed one ultra-low attachment (ULA) 96-well plate of embryoid bodies. To passage the cells, mTeSR was aspirated and the cells washed with PBS. 1 mL of Accutase was then added to the well and incubated at 37 °C incubator for 4-6 minutes. Cells were detached by tapping the sides of the plate. 1 mL of mTesr was then added to the well, and the detached cells were titurated with a 200 µl pipette to break up cell clumps and to obtain a single cell suspension. Cells were then spun down at 300 rcf for 5 minutes. Once the cells were pelleted, , the supernatant was removed, and cells resuspended in EB medium - (DMEM-F12, 20% KOSR) + 50 µM Y-27632 - at a concentration of 72,000 cells/ml. 125 µL of this cell suspension, was dispensed into each well of an ULA 96 well plate. hESCs were cultured overnight at 37 ºC, 5% CO_2, allowing them to aggregate into embryoid bodies (EBs).

EBs were grown for 1-3 days till 200-400 µm in diameter. Once this size, EBs were transferred into an ULA 6-well plate using a cut 200 µL pipette tip, with a maximum of ~24 EBs per well of the ULA 6 well plate. Excess EB medium was carefully removed and 2 mL of Mesoderm Induction Media: N2/B27 medium - (1:1 DMEM/F12-Neurobasal, 100x N2, 50x B27) - + 3 µM CHIR (Tocris), 30 ng/mL BMP4 (Peprotech), 1 µg/ml of doxycycline (dox); was added to each well. These were then cultured at 37 ºC, 5% CO_2 for 3 days.

Three days later, the medium was replaced with 2 mL of Vascular Induction Media: N2/B27 medium + 100 ng/ml VEGF (Peprotech) + 10 µM Forskolin (Sigma-Aldrich) + 1 µg/ml dox per

well; and cultured at 37 ºC, 5% CO_2. 24 hours later, medium was removed and replaced with 2 mL of N2/B27 media + 100 ng/ml VEGF + 10 µM Forskolin + 1 µg/ml dox per well. Organoids were then cultured at 37 ºC, 5% CO_2 for 24 hours.

Organoids were then encapsulated in a blend of matrigel and collagen (Mat-Col gel: 2 mg/mL Collagen (Advanced Biomatrix) + 20% Matrigel). Briefly, parafilm wells were prepared by placing a piece of parafilm onto an empty 200 µL pipette tip box, and pressing into the tip cavities to create dimples. A 7 x 7 grid of wells was found to be optimal since it prevented organoids from drying and allowed sufficient organoids to be encapsulated for culturing in one 10 cm dish. The dimpled parafilm was then placed in a 10 cm dish. The Mat-Col Gel Blend was prepared and placed on ice.

Using a cut 200 µL pipette tip, organoids were transferred from the ULA 6 well plate, and placed individually into the parafilm wells. A maximum of ~30 µL of media was transferred with each organoid to avoid overfilling of the parafilm well. Once all organoids were placed in individual wells, excess media was removed, leaving only the organoid in the well. 30 µL of the Mat-Col gel was added to each parafilm well. Individual organoids were checked to ensure encapsulation in the gel solution, and the 10 cm dish was then incubated at 37 ºC, 5% CO_2 for 45 minutes for the gel blend to completely gelate.

Once gelation was complete, the encapsulated organoids were washed off the parafilm using Vascular Maturation Media: StemPro 34 Media + 15% FBS + 100 ng/ml VEGF + 100 ng/ml bFGF + 1 µg/ml dox. Once gel droplets were completely washed off from the parafilm, a cut 1000 µL pipette tip was used to transfer the organoids back to the original ULA 6 well plate used in the previous steps of the experiment. Organoids were then cultured at 37 ºC, 5% CO_2 and medium replaced every 3 days using Vascular Maturation Media until day 15.

For long term culture of iN-VOs, at day 15, medium was changed to Vascular Maturation Media + 20 ng/ml BDNF + 20 ng/ml NT3 + 1 µg/ml dox. Medium was replaced every 3-5 days.

Animals

Housing, husbandry and all procedures involving animals used in this study were performed in compliance with protocols (#S16003) approved by the University of California San Diego Institutional Animal Care and Use Committee (UCSD IACUC). Mice were group housed (up to 4 animals per cage) on a 12:12 hr light-dark cycle, with free access to food and water in individually ventilated specific pathogen free (SPF) cages. All mice used were healthy and were not involved in any previous procedures nor drug treatment unless indicated otherwise. All studies performed in NOD.Cg-Prkdcscid Il2rgtm1Wjl/SzJ (NSG) mice and maintained in autoclaved cages.

In Vivo Perfusion

iN-VOs were cultured for 30 days before being implanted subcutaneously into $Rag2^{-/-};\gamma c^{-/-}$ immunodeficient mice. To prepare the mice for subcutaneous implantation, the right hind-flank region was shaved and wiped down with povidone-iodine. Then, a one-inch, subcutaneous incision was made, and Day 30 iN-VOs suspended in Matrigel were placed inside the incision region using a cut pipette tip. These organoids were then matured for an extra 30 days in-vivo. To test for proper perfusion of the vasculature, mice were given an intravenous injection of lysine fixable Texas-Red Dextran (1.25 mg per mouse, Thermo Fisher Scientific) and sacrificed after 15 minutes of allowing the dextran to pass through circulation. Organoids were retrieved from the subcutaneous region, fixed and whole-mount stained, as described below.

MEA Measurements

For 2D differentiated neurons, cells were plated on Matrigel coated 6-well multi-electrode arrays (CytoView MEA 6, Axion Biosystems) with mouse glial cells and maintained in culture for up to 3 weeks.

iN-VOs were not encapsulated in Mat-Col gel when preparing them for MEA measurements. MEA electrodes (CytoView MEA 6, Axion Biosystems) were spot-coated with 2% Matrigel and placed in a cell-culture incubator to incubate at 37 ℃ overnight. Because gel encapsulation prevented proper adhesion between the organoid and MEA well, the following day, one day-25 un-encapsulated iN-VO was carefully put in the center of the MEA well with ~50 μL of media. The organoid was left untouched for 2 hours, and then flooded with 0.5 mL of media. PBS was filled in the side compartments of the MEA plate to prevent cell media evaporation. The MEA plates were then left undisturbed for 5 days to ensure robust attachment to the well. MEA measurements were taken on day 30, 5 days after seeded onto the plate. To collect measurements, MEA plates were placed in the reader with the reader plate heater set to 37 ºC and under 95% O_2/5% CO_2 air flow. Plates were allowed to equilibrate under these conditions for a minimum of 5 minutes before collecting spontaneous recordings for 4 minutes.

Electrical signals were collected and analyzed using AxIS Software (Axion Biosystems) with Spontaneous Neural configuration. Signals were filtered with a band-pass filter of 200 Hz – 3 kHz. Spikes were detected with AxIS software using an adaptive threshold crossing set to 5.5 times the standard deviation of the estimated noise for each electrode.

In vitro electrical stimulation

To create chambers for electrical stimulation, custom designed chips consisting of a porous inner well and a solid outer well were fabricated via extrusion printing of a silicone elastomer (Dow Corning Dowsil SE 1700) on glass slides, on a custom 3D printer consisting of a three-axis gantry

(AGB 10000, Aerotech) and pneumatic dispensers (Nordson Ultimus I). Chips were cured for at least two hours at 80 ºC to fully crosslink the elastomer. Graphite rods were then inserted into these chips such that they were located at either end of the inner well and gaps were sealed with PDMS (Dow Corning, Sylgard 184). After sealing, chips were again cured for at least two hours at 80 ºC.

To encapsulate iMB-VOs, a solution composed of Fibrin (3 mg/ml, Sigma Aldrich) + 20% Matrigel was prepared similarly to a previously described protocol (Rao et al. 2018). Up to five individual organoids were transferred into the inner well, excess medium removed and the space filled with the hydrogel mixed with thrombin (1 U/ml, Sigma-Aldrich). The hydrogel was allowed to fully gelate and crosslink at 37 ºC for one hour, after which the outer well was filled with VO culture medium containing 1 µg/ml dox. For stimulated samples, wires were attached to the graphite rods and routed to Arduino Uno microcontrollers equipped with Motor Shields. The microcontrollers were programmed to provide chronic electrical stimulation at 0.4 V/mm, 1 Hz with a 2 ms on time. Encapsulated organoids were then cultured in 37 ºC, 5% CO_2 for eight days. On the second day after encapsulation, electrical stimulation was started and maintained for one week.

Immunostaining

Organoids were removed from the culture dish and added to a 1.5 mL centrifuge tube. Up to 20 organoids could be combined into one tube and used in subsequent steps. Excess medium was removed and organoids were washed once with 1 mL PBS. PBS was removed and 500 μL of 4% PFA solution was added to the microcentrifuge tube. Organoids were fixed at room temperature for 1 hour, protected from light. After 1 hour, PFA solution was removed and exchanged with 500 µL PBS. At this point, organoids could be stored in PBS at 4 °C protected from light for up to 1 month.

To block the organoids, and prepare them for immunostaining, PBS was removed and 500 µL of blocking buffer (3% FBS, 1% BSA, 0.5% Triton-X, 0.5% Tween) was added. The tube was placed into a tube rack and then onto an orbital shaker, shaking at 150 rpm for 2 hours to fully block and permeabilize the organoids. Blocking buffer was then removed and 100 µL of primary antibody diluted in blocking buffer was added. All antibodies used were diluted 1:100 in blocking buffer. The tube then was placed back onto the tube rack and onto an orbital shaker (LSE Orbital Shaker, Corning) at 4 °C. The orbital shaker was set to 12 rpm and organoids incubated at 4 °C overnight.

After overnight incubation, blocking buffer was removed, and organoids washed with PBS-T (PBS + 0.05% Tween) three times for 20 minutes. Organoids were placed on an orbital shaker set to 150 rpm during each PBS-T wash.

After washing in PBS-T, 100 µL of secondary antibodies diluted in blocking buffer were added. Organoids were incubated with the secondary antibodies at room temperature for 2 hours, while keeping the samples protected from light. After secondary staining was complete, organoids were washed with PBS-T three times for 20 minutes. Organoids were placed on an orbital shaker set to 150 rpm during each PBS-T wash.

Once secondary staining was complete, a coverslip was prepared for whole-mounting of the organoids. This was done by applying epoxy (Loctite Epoxy) to the non-adhesive surface of an iSpacer (Sunjin Lab) and then attaching the iSpacer to a coverslip. Within 5 minutes the iSpacer was bound to the coverslip. Using a cut 1000 µL pipette tip, 2-4 organoids were transferred to each iSpacer well. Excess PBS was removed and 50 µL of Fluromount G was added to each well. iSpacer cover was then peeled off and a second coverslip attached the exposed sticky side. Whole-mount samples could be stored in 4 °C protected from light for up to 8 months. Confocal images were taken using a LSM 880 with Airyscan Confocal Microscope (Zeiss).

All of the Primary and Secondary Antibodies used in this protocol are diluted in Blocking Buffer at a 1:100 dilution factor. anti-VE-Cadherin (D87F2, Cell Signaling Technologies), anti-MAP2 (HM-2, Sigma-Aldrich), anti-MYH (MF-20, DSHB), anti-PDGFR (AF385, R&D Systems) and anti-SMA (MAB1420, R&D Systems) were used for primary antibody staining. anti-Rabbit Alexa 405 (Thermo Fisher Scientific, A-31556), anti-Rabbit DyLight 550 (Thermo Fisher Scientific, 84541), and anti-Mouse Alexa 647 (Thermo Fisher Scientific, PIA32728) were used for secondary antibody staining.

For endothelial function Dil–acetylated low-density lipoprotein (Dil-ac-LDL) uptake assay, neuro-vascular organoids were incubated with with 10 μg ml−1 Dil-ac-LDL (Thermofisher, L3484) for 6 hours and then washed several times in medium before immunostaining and imaging.

RNA Extraction and qRT-PCR

RNA was extracted from cells using the Qiazol and RNeasy Mini Kit (Qiagen) as per the manufacturer's instructions. The quality and concentration of the RNA samples was measured using a spectrophotometer (Nanodrop 2000, Thermo Fisher Scientific). cDNA was prepared using the Protoscript II First Strand cDNA synthesis kit (New England Biolabs) in a 20 μl reaction and diluted up to 1:2 with nuclease-free water.

qRT-PCR reactions were setup as: 2 μl cDNA, 400 nM of each primer, 2X iTaq Universal SYBR Supermix (Bio-Rad), H2O up to 20 μl. qRT-PCR was performed using a CFX Connect Real Time PCR Detection System (Bio-Rad) with the thermocycling parameters: 95 °C for 3 min; 95 °C for 3 s; 60 °C for 20 s, for 40 cycles. All experiments were performed in triplicate and results were

normalized against a housekeeping gene, GAPDH. Relative mRNA expression levels, compared with GAPDH, were determined by the comparative cycle threshold ($\Delta\Delta C_T$) method.

The following primers were used for qPCR reactions:

MAP2 Forward primer	CTCAGCACCGCTAACAGAGG
MAP2 Reverse primer	CATTGGCGCTTCGGACAAG
TUBB3 Forward primer	GGCCAAGGGTCACTACACG
TUBB3 Reverse primer	GCAGTCGCAGTTTTCACACTC
VGLUT2 Forward primer	GGGAGACAATCGAGCTGACG
VGLUT2 Reverse primer	TGCAGCGGATACCGAAGGA
VGAT Forward primer	ACGTCCGTGTCCAACAAGTC
VGAT Reverse primer	AAAGTCGAGGTCGTCGCAATG
BRN2 Forward primer	AAGCGGAAAAAGCGGACCT
BRN2 Reverse primer	GTGTGGTGGAGTGTCCCTAC
FOXG1 Forward primer	CCGCACCCGTCAATGACTT
FOXG1 Reverse primer	CCGTCGTAAAACTTGGCAAAG
CDH5 Forward primer	AAGCGTGAGTCGCAAGAATG
CDH5 Reverse primer	TCTCCAGGTTTTCGCCAGTG
VEPTP Forward primer	ACAACACCACATACGGATGTAAC

VEPTP Reverse primer	CCTAGCAGGAGGTAAAGGATCT
SMA Forward primer	GTGTTGCCCCTGAAGAGCAT
SMA Reverse primer	GCTGGGACATTGAAAGTCTCA
MYH1 Forward Primer	ATCTAACTGCTGAAAGGTGACC
MYH1 Reverse Primer	TAAGTAAATGGAGTGACAAAG
MYH2 Forward Primer	GCCGAGTCCCAGGTCAACAAG
MYH2 Reverse Primer	TGAGCAGATCAAGATGTGGCAAAG
MYH7 Forward Primer	CTGTCCAAGTTCCGCAAGGT
MYH7 Reverse Primer	TCATTCAAGCCCTTCGTGCC
CASQ1 Forward Primer	ACATTGTGGCCTTCGCAGAG
CASQ1 Reverse Primer	CCATACGCTATCCGCATCAGT
SERCA1 Forward Primer	GAAGGGAGCACAATGGAGGC
SERCA1 Reverse Primer	CAGGCCAGCACGAAGGAAAT

Statistics

All statistics on gene expression qPCR plots were assayed via an unpaired two-tailed t-test. P values were assessed as significant as follows: $^{**}P \leq 0.01$, $^{***}P \leq 0.001$, and $^{****}P \leq 0.0001$; ns = not significant. Statistical analysis was carried out using GraphPad Prism 8.

Single cell RNA-seq Processing

To dissociate organoids for single cell RNA-seq, 5-6 organoids were incubated in a 1 mL 20 U/mL Papain solution (Worthington, LS003126) for 30 minutes, passed through a 40 μm filter, spun down at 300 rcf for 5 minutes, and resuspended in 0.04% BSA solution. Cells were then loaded into the Chromium Chip B (10x Genomics) and single cell libraries were made using Chromium Single Cell 3' Reagent Kits v3 workflow (10x Genomics). Fastq files were aligned to a hg19 reference and expression matrices generated using the count command in cellranger v3.0.1 (10X Genomics).

Data Integration and Clustering

Data integration was performed on the expression matrices from all 3 organoids: iN-VOs induced for 15 days; iN-VOs induced for 45 days; and iN-VOs which were not induced. Integration was done using the Seurat v3 pipeline (Butler et al. 2018). Expression matrices were filtered to remove any cells expressing less than 200 genes or expressing greater than 10% mitochondrial genes. DoubletFinder (McGinnis, Murrow, and Gartner 2019) was used to detect predicted doublets, and these were removed for downstream analysis. The expression matrix was then normalized for total counts, log transformed and scaled by a factor of 10,000 for each sample, and the top 4000 most variable genes were identified. We then used Seurat to find anchor cells and integrated all data sets, obtaining a batch-corrected expression matrix for subsequent processing. This expression matrix was scaled, and nUMI as well as mitochondrial gene fraction was regressed out. Principal component analysis (PCA) was performed on this matrix and 22 PCs were identified as significant using an elbow plot. The 22 significant PCs were then used to generate a k-nearest neighbors (kNN) graph with k=10. The kNN graph was then used to generate a shared nearest neighbors (sNN) graph followed by modularity optimization to find clusters with a resolution parameter of 0.8.

To classify cell types, the integrated dataset was mapped to annotated cell types in the Microwell-seq Mouse Cell Atlas (Han et al. 2018) using Seurat label transfer on the intersection of genes in the mouse and organoid datasets, and further refined using cell type-specific marker genes. We finally visualized the results using UMAP dimensionality reduction on the first 22 PCs.

To assess tissue-specificity of endothelial cells, the endothelial cell cluster was subsetted and mapped using Seurat label transfer to tissue-specific endothelial cells from the Tabula Muris consortium. To confirm neuronal character of neurons from the neurovascular organoids, the neuron cluster was subsetted and mapped via Seurat label transfer to cells profiled during differentiation of neurons from pluripotent stem cells in 2D using *NGN2* overexpression. For all mapping to a reference data set, the prediction score is assessed as the mean of the Seurat predicted identity score across all cells with a particular identity.

SUPPLEMENTAL NOTES

Note S1: Optimization of organoid composition cell ratio

We sought to assess whether iN hESCs would differentiate to neurons when *NEUROD1* expression was induced by doxycycline under the culture conditions of vascular organoid differentiation. Since we did not know a priori if all iN cells would differentiate to neurons and disrupt formation of vascular networks in the organoid, we first tested induced neuro-vascular organoid (iN-VO) formation with two ratios of iN:Wild-Type (WT) cells, either 100% iN cells or a mix of 50% iN cells and 50% WT cells (**Figure S1a**). Induced organoids (+dox conditions) for both cell ratios showed a marked increase in *MAP2* expression, with expression levels 4- to 8-times higher compared to uninduced organoids (-dox conditions) (**Figure S1b**), suggesting robust neuronal differentiation under dox induction.

Note S2: Optimization of neuro-vascular organoid media conditions for long-term organoid growth

When cultured in standard VO vascular organoid media conditions, neuronal survival was compromised and by day 30 there was no observable *MAP2* expression in induced organoids compared to uninduced organoids (**Figure S1f**). To enhance the long term survival of neurons in the organoids, we tested supplementing with the growth factors BDNF and NT-3, and as well as the neuronal cell culture supplement B-27. Supplements were added to the culture from day 15 onward, and organoids were assayed at day 30. In addition, we tested whether continued overexpression of *NEUROD1* beyond day 15 may lead to impaired neuronal survival by including conditions where doxycycline was removed from culture after day 15. All organoids were assayed at day 30 by qRT-PCR for *MAP2* and *CDH5* expression. We observed highest *MAP2* expression in organoids where doxycycline was retained in the medium till day 30, and the medium was supplemented with BDNF and NT-3, about 10-times higher than uninduced organoids (**Figure**

S1f), while maintaining similar *CDH5* expression as uninduced organoids. Thus, for subsequent long-term experiments we supplemented the culture medium with BDNF and NT-3 from day 15 onward to ensure long term survival of neurons with reliable maintenance of vascular lineages.

REFERENCES

Albini, Sonia, Paula Coutinho, Barbora Malecova, Lorenzo Giordani, Alex Savchenko, Sonia Vanina Forcales, and Pier Lorenzo Puri. 2013. “Epigenetic Reprogramming of Human Embryonic Stem Cells into Skeletal Muscle Cells and Generation of Contractile Myospheres.” *Cell Reports* 3 (3): 661–70.

Butler, Andrew, Paul Hoffman, Peter Smibert, Efthymia Papalexi, and Rahul Satija. 2018. “Integrating Single-Cell Transcriptomic Data across Different Conditions, Technologies, and Species.” *Nature Biotechnology* 36 (5): 411–20.

Han, Xiaoping, Renying Wang, Yincong Zhou, Lijiang Fei, Huiyu Sun, Shujing Lai, Assieh Saadatpour, et al. 2018. “Mapping the Mouse Cell Atlas by Microwell-Seq.” *Cell* 172 (5): 1091–1107.e17.

Liu, X. Shawn, Hao Wu, Xiong Ji, Yonatan Stelzer, Xuebing Wu, Szymon Czauderna, Jian Shu, Daniel Dadon, Richard A. Young, and Rudolf Jaenisch. 2016. “Editing DNA Methylation in the Mammalian Genome.” *Cell* 167 (1): 233–47.e17.

McGinnis, Christopher S., Lyndsay M. Murrow, and Zev J. Gartner. 2019. “DoubletFinder: Doublet Detection in Single-Cell RNA Sequencing Data Using Artificial Nearest Neighbors.” *Cell Systems* 8 (4): 329–37.e4.

Paik, David T., Lei Tian, Ian M. Williams, Siyeon Rhee, Hao Zhang, Chun Liu, Ridhima Mishra, Sean M. Wu, Kristy Red-Horse, and Joseph C. Wu. 2020. “Single-Cell RNA Sequencing Unveils Unique Transcriptomic Signatures of Organ-Specific Endothelial Cells.” *Circulation* 142 (19): 1848–62.

Rao, Lingjun, Ying Qian, Alastair Khodabukus, Thomas Ribar, and Nenad Bursac. 2018. “Engineering Human Pluripotent Stem Cells into a Functional Skeletal Muscle Tissue.” *Nature Communications* 9 (1): 126.

Schörnig, Maria, Xiangchun Ju, Luise Fast, Sebastian Ebert, Anne Weigert, Sabina Kanton,

Theresa Schaffer, et al. 2021. “Comparison of Induced Neurons Reveals Slower Structural and Functional Maturation in Humans than in Apes.” *eLife* 10 (January). https://doi.org/10.7554/eLife.59323.

Victor, Matheus B., Michelle Richner, Tracey O. Hermanstyne, Joseph L. Ransdell, Courtney Sobieski, Pan-Yue Deng, Vitaly A. Klyachko, Jeanne M. Nerbonne, and Andrew S. Yoo. 2014. “Generation of Human Striatal Neurons by microRNA-Dependent Direct Conversion of Fibroblasts.” *Neuron* 84 (2): 311–23.

Wang, W., Y. Xue, S. Zhou, A. Kuo, B. R. Cairns, and G. R. Crabtree. 1996. “Diversity and Specialization of Mammalian SWI/SNF Complexes.” *Genes & Development* 10 (17): 2117–30.

Yang, Nan, Soham Chanda, Samuele Marro, Yi-Han Ng, Justyna A. Janas, Daniel Haag, Cheen Euong Ang, et al. 2017. “Generation of Pure GABAergic Neurons by Transcription Factor Programming.” *Nature Methods* 14 (6): 621–28.

Yusa, Kosuke, Liqin Zhou, Meng Amy Li, Allan Bradley, and Nancy L. Craig. 2011. “A Hyperactive piggyBac Transposase for Mammalian Applications.” *Proceedings of the National Academy of Sciences of the United States of America* 108 (4): 1531–36.

Zhang, Yingsha, Changhui Pak, Yan Han, Henrik Ahlenius, Zhenjie Zhang, Soham Chanda, Samuele Marro, et al. 2013. “Rapid Single-Step Induction of Functional Neurons from Human Pluripotent Stem Cells.” *Neuron* 78 (5): 785–98.